

## FIELD MEASUREMENTS OF SNOWDRIFT DEVELOPMENT RATE

R.B. Haehnel<sup>1</sup>, J.H. Lever<sup>1</sup> and R.D. Tabler<sup>2</sup>

### ABSTRACT

For successful snow drift modeling, similitude of drift geometry and development rate must be preserved between model and prototype. Earlier work revealed that field data documenting drift development are scarce, yet such data are necessary to validate proposed modeling methods. This requires measurement of the evolving drift topography and concurrent measurement of the incident mass transport and flow field throughout the drifting event. The authors established a field program to measure drift development on a two-dimensional solid fence during the winters of 1996 and 1997 at two field sites located in Wyoming. The developing drift topography was measured using graduated snow stakes placed around the objects. The incident mass transport was measured using a Wyoming snow fence as a snow trap. The incident flow field was also documented.

Here we compare prototype drift geometries and development rates with corresponding preliminary model data obtained in a snow drifting wind tunnel. The field data revealed some inaccuracies in the model drift geometry and development rate which might result from distortion in snow transport concentration and particle trajectory lengths. Further work is required to minimize the effects of model distortions. The field data obtained in this work will serve as benchmark data for evaluating modeling methodologies.

### INTRODUCTION

Successful snow drift modeling requires similitude of the drift geometry and development rate between model and prototype. This in turn requires similitude of the governing forces that drive drift development. Works by Strom et al. (1962), Odar (1965), Kind (1976, 1986), Weubben (1978), Iversen (1979, 1980), Anno (1984), Isyumov et al. (1989), Kwok et al. (1992) and others show consensus on appropriate similitude requirements, except in the manner to scale snow drift development rates. This problem persists because practical physical modeling necessitates the distortion of some important similitude parameters, and the impact of these distortions on the time-scale is unclear. Furthermore, good field data to validate proposed model formulations are scarce.

Recent work presented by Smedley et al. (1993) and Lever and Haehnel (1995) show good agreement between model and prototype drift development rates for an elevated building and a Wyoming snow fence, respectively. In each case the time-scale is based on scaled snow mass transport as originally proposed by Anno (1984):

$$Q' = \frac{qt}{\rho_b L^2} \quad (1)$$

where,  $Q'$  is the dimensionless mass transport rate,  $q$  is the snow mass flux,  $t$  is elapsed time,  $\rho_b$  is the snowdrift bulk density and  $L$  is the characteristic length. However, snow particles pass under an elevated building or through a snow fence to arrive in the low velocity wake. Consequently, there can be considerable distortion in particle trajectory length and height of the snow transport layer between model and prototype without major impacts on the delivery of particles into the wake region behind these porous structures. Thus, these structures may not provide very demanding tests of the validity of Anno's time-scale formulation.

A more demanding structure would be a solid object such as a building or a wall where the snow particles are forced to go over or around the object in order to reach the wake region. Lever and Haehnel (1995) show that distortions in the model can result in model particles trajectories that are proportionally longer (compared to the structure dimensions) than in the prototype. Model particles may thus overshoot a wake region that field particles would fall into. The similitude parameter typically associated with particle trajectory length is the ratio between the particle inertia and gravitation force, or the Froude number,  $Fr$ ,

$$Fr = \frac{U^2}{gL} \quad (2)$$

where  $U$  is the free stream velocity and  $g$  is the gravitational constant. Long particle trajectories are reflected in Froude numbers that are too high in the model in comparison to the field. We expect that Froude distortion would

<sup>1</sup> Cold Regions Research and Engineering Laboratory, 72 Lyme Rd., Hanover, NH 03755-1290, USA.

<sup>2</sup> Tabler and Associates, 7505 Estate Circle, Niwot, CO 80544-0483, USA.

lead to lower capture efficiencies and drift development rates in the model than is demonstrated in the field. The extent to which Froude distortion impacts model drift development rates has not been fully addressed to date, principally due to a lack of field data that documents drift development on solid objects.

In this work we compare the drift development rate between the model and prototype for a two-dimensional solid fence. The fence is simple to construct in the field, yet as a solid structure this geometry will probe the limitations of wind tunnel modeling. The developing snow drift on a 1.22m tall solid fence was measured at two sites in Wyoming, and these tests were replicated in CRREL's wind tunnel facility on a 1:12 scale model of the fence.

### EXPERIMENTAL PROCEDURE

Documenting drift development rate requires measurement of the developing drift geometry accompanied by measurements of the incident mass transport and flow field (Haehnel and Lever, in press). Below we outline our approach to accomplish this in the field and laboratory.

#### Field measurements

Field measurements of the drift development on a two-dimensional solid fence were taken at two field sites located along Wyoming Interstate 80 during the winters of 1995 and 1996. These sites were chosen since these areas are relatively flat, frequently experience heavy snow drifting and already had snow fences installed. During the winter of 1995-96 the study site was located at mile 255 on I-80 near Elk Mountain (N 41° 43.623', W 106° 28.432'). During the winter of 1996-97 the study site was located at the Cooper Cove interchange, mile 280.5 on I-80 (N 41° 32.008', W 106° 4.751'). In both instances 1.22 m tall, 29m long solid fences were installed with the long axis normal to the prevailing wind direction. The wind speed at 1.5, 2.5 and 4.5 m heights, and wind direction at 4.5 m was measured throughout the winter. In addition to recording the 15 minute average wind speed at 4.5m, the instantaneous wind speed at each height was also recorded every 15 minutes. These instantaneous measurements were used to calculate the friction velocity of the incident flow field. Additionally, the air temperature, atmospheric pressure, and incoming short-wave solar radiation was measured throughout the winter.

To measure the snow drift depth on the solid fence, three rows of 1.22 m tall graduated snow stakes were installed on the windward and leeward sides of the fence. The rows of snow stakes ran perpendicular to the snow fence. The stakes were marked with 5 cm graduations and were spaced 1.1 m apart. On the windward side the rows were 9.14 m long, on the leeward side the rows were 15.5 m long. The rows were 3 m apart, with the center row located at the center of the fence.

The snow mass transport was measured using the available "Wyoming" style snow fences. These had also been installed with the long axis normal to the prevailing wind. The Elk Mountain site used a single 3.66 m snow fence to measure the mass transport. Tabler and Jairell (1993) showed that a 2.44 m Wyoming snow fence is effective at capturing about 95% of the incident blowing snow until the fence is filled to about 20 % of its capacity. We assume that the 3.66 m fence has approximately the same capture efficiency,  $\eta$ , as that of the 2.44 m fence. The mass flux (mass per unit time per unit lane width),  $q$ , is then the added volume of the snow drift on the fence per unit lane width,  $\Delta V/w$ , times the bulk density of the drift. Assuming the drift shape is two-dimensional then the volume is the drift cross-sectional area,  $A$ , times the width,  $w$ , so the mass transport is

$$q = \frac{\rho_b A}{\eta t} \quad (3)$$

At the Cooper Cove site the mass transport was measured using two fences in tandem with a 2.44m snow fence located 61m directly upwind of a 3.8 m snow fence. In this case the small amount of blowing snow that passes the 2.44 m fence is captured by the 3.8 m fence. Thus, the capture efficiency for this system is 100% (Tabler and Jairell, 1993), and the area used in equation (2) is the combined added area for the two snow fences. If we take the characteristic length,  $L$ , to be the height of the solid fence,  $h$ , and combine equations (1) and (3) we find the non-dimensional mass transport is simply

$$Q' = \frac{A}{\eta h^2} \quad (4)$$

The snowdrift topography on the snow fences was measured by taking transverse cross-sections perpendicular to the snow fence using a snow probe. Measurements were taken at 1.52m intervals.

A typical test proceeded as follows. Just prior to a forecasted drifting snow event the 1.22 m tall x 29 m long solid fence was installed and the initial snow depth around the solid fence and the snow fence was recorded. Once the blowing snow event began, successive measurements of the snow topography on the solid fence and the snow fence were taken until the event subsided, or the equilibrium drift was reached.

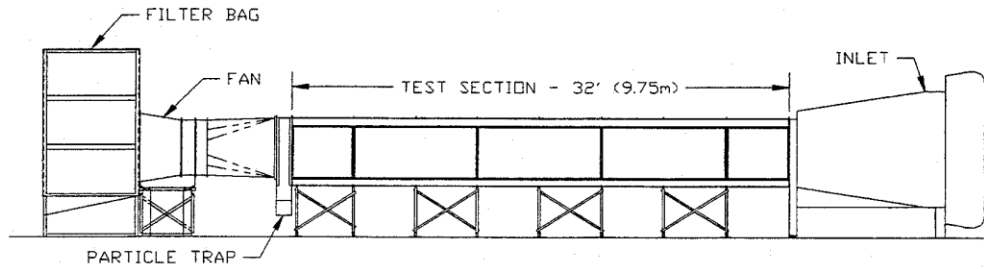


Figure 1. Schematic of CRREL Environmental Wind Tunnel.

#### Wind tunnel measurements

The model test was conducted in CRREL's Environmental Wind Tunnel (fig. 1). This is an open circuit boundary layer wind tunnel used for modeling snow drifting and has a 2.44 m (8 ft) wide x 1.22m (4 ft.) high cross-section with a 9.75 m (32 ft) long the test section. The maximum wind speed is 11 m/s. The snow is simulated using spherical glass beads which have a mean diameter of 80  $\mu\text{m}$  and a density of 2.44g/cm<sup>3</sup> (Haehnel et al., 1993). The mass transport is measured by capturing the beads in the particle trap and filter bag. The wind speed was measured using a pitot tube manometer.

The incident flow field over a saltating bead surface can be characterized as fully developed neutrally stable turbulent boundary layer flow and has a velocity profile which can be characterized as

$$\frac{U_z}{u_*} = \frac{1}{k} \log\left(\frac{z}{Z_o'}\right) \quad (5)$$

where  $U_z$  is the velocity at height  $z$ ,  $u_*$  is the friction velocity,  $k$  is von Karman's constant ( $k = 0.4$ ),  $Z_o'$  is the aerodynamic roughness height for saltation. The values measured in the wind tunnel for  $Z_o'$  for saltating beads is 0.034 - 0.069mm. Field measurements of  $Z_o'$  over snow range from 0.12 - 5.8mm (Mellor, 1965) which is 3- 83 times greater than the model, which suggests the flow field in the wind tunnel will be suitable for modeling structures at scales of 3 - 80.

The model solid fence we tested in the wind tunnel was 10.4 cm tall corresponding to 1:12 scale. The initial snow depth conditions were established by grading the beads to a uniform depth both up wind and down wind of fence. The up wind snow field extended 5m in front of the fence. This allowed a fully developed turbulent boundary layer to develop over the snow field prior to encountering the area of interest. The test was run at a free-stream velocity of 5m/s. To document the drift development the test was stopped at intermediate points and the drift topography was measured at three transverse cross-sections spaced 0.5 m apart using a snow probe. Also at this time, additional snow was added to the upstream fetch to restore the snow surface to its original depth and we measured the mass of snow captured in the particle trap and filter bag. The cross-sections were then plotted and the test resumed.

The mass transport was determined by adding the mass of beads caught in the particle trap and filter bag to the mass of beads deposited on the solid fence. The mass of beads deposited on the solid fence was determined by calculating the volume from the drift topography and multiplying that by the bulk density of the beads. Using this information, the non-dimensional mass transport was calculated using equation (1).

## RESULTS

During the two winters in the field we were able to measure five separate drift events. Of these, two reached equilibrium. The remaining three events did not reach equilibrium either due to exhaustion of the snow supply or the ambient temperature exceeding freezing and causing melting of the snow. For every drifting event the wind direction was predominantly from the prevailing direction for that site. Typical wind speeds during these events ranged from 8 - 15 m/s (2 - 3 times the threshold speed). The one event logged at the Elk Mountain site had wind speeds ranging from 10 - 15 m/s, while the remaining 4 events that were measured at the Cooper Cove site had wind speeds ranging from 8 - 12 m/s. As previously stated, the model wind speed was about 5 m/s or 1.25 times the threshold speed. At a model scale of 1:12 the model Froude number was about twice as large as the average prototype Froude number.

Typical profiles of the drift on the solid fence for both the field and model are shown in figure 2. The numbering of the curves indicate the sequence of the drift evolution. The windward drift for both the model and prototype are almost identical (fig 2a). From figure 2b we find the leeward drift in the model is about twice as long as the field case, yet in all other respects closely mimics the field. Since the equilibrium drift was not reached in the model we show the postulated equilibrium drift shape with a dashed line. For both the windward and leeward drifts we find the model drift is more rounded at its intermediate stages than is observed in the field. One might expect this since the beads are cohesionless particles that have dynamic and static angles of repose of about  $19^\circ$  and  $32^\circ$ , respectively. Therefore the beads cannot preserve the steep features exhibited by natural snow. The steepest angles achieved on the windward and leeward drifts were  $18^\circ$  and  $13^\circ$ , respectively.

The increase in drift cross-sectional area with increasing snow drift transport for both the model and field is shown in figure 3. The field data is indicated by the symbols, while the model data is indicated by the solid line. Extrapolated model data is indicated by the dashed line. We compare the drift development rate of the total drift area between model and prototype in figure 3a. For comparison we have also included the expected drift evolution for a Wyoming snow fence (assuming the capture efficiency is 95%). In general the results for the model and prototype agree very well. Furthermore, we find that the capture efficiency of a solid fence is essentially equal to that of a snow fence during early stages of drift development ( $Q' < 3$ ) for both the model and prototype. In the prototype case we find the drift continues to develop at the same rate as the snow fence for  $Q' > 3$  until it approaches equilibrium. However, for  $Q' > 3$  the model drift does not grow as rapidly as the field case or the snow fence.

From figure 3b we see the windward drift develops more rapidly in the wind tunnel than in the field. Furthermore, the model drift exhibits a constant rate of growth until it reaches equilibrium. The field drift initially grows at a constant rate, but as it nears equilibrium the drift area actually overshoots the equilibrium size and then erodes back some before settling in to a final equilibrium area. We observe that the equilibrium drift area for both the model and field is about  $2.3 - 2.4 A/H^2$ .

In contrast we find the leeward drift in the model does not even begin to grow until  $Q'$  is about 2 to 2.5, yet the field drift shows steady growth from the onset of drifting. However, once the model drift does begin to develop its area increases at virtually the same rate as the field. We note when the windward drift in the model reaches equilibrium ( $Q' \sim 3$ ) is nearly the same time that the leeward drift in the model starts to develop. We ran out of snow supply in the model at about the time the leeward model drift reached the same area as the field drift at equilibrium ( $2.8 - 3 A/h^2$ ). However, the model drift apparently had not reached equilibrium. We expect the final drift area for the model would be about  $6 A/h^2$  as indicated by the dashed line in figure 3c. This would be about twice the cross-sectional area of the field drift.

## DISCUSSION OF RESULTS

The field measurements of drift development were very repeatable, with the data showing very little scatter. From figures 2 and 3 we observe many similarities between the model and prototype drifts for a solid fence, yet there are two important differences that cannot be overlooked: the model leeward drift does not develop early enough, and when it does develop, it is too large.

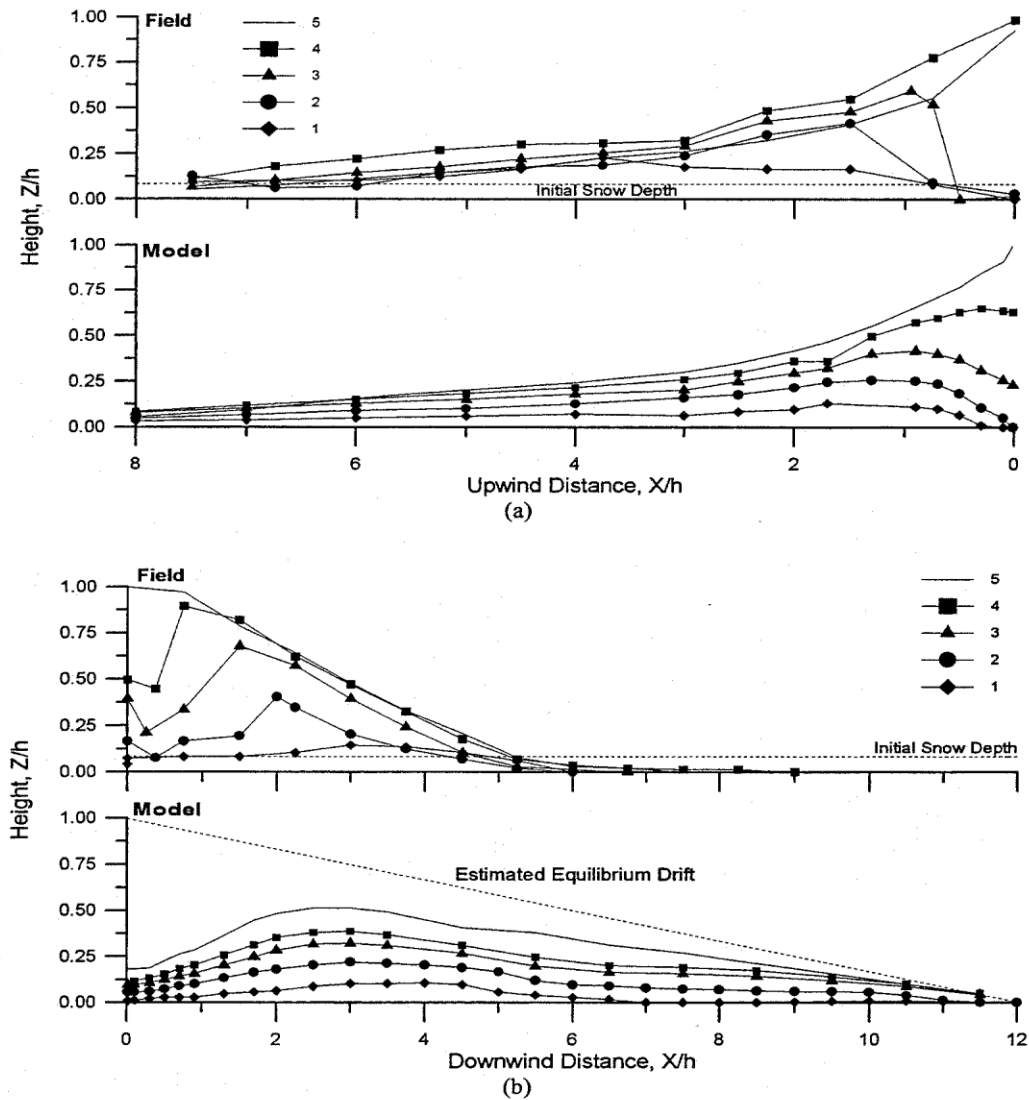
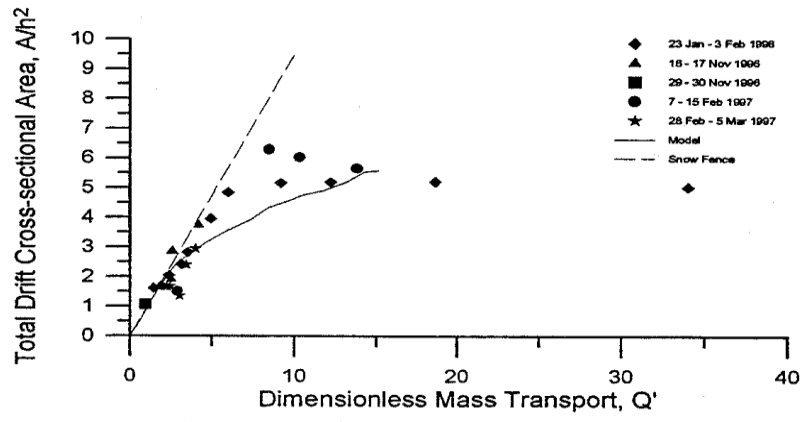


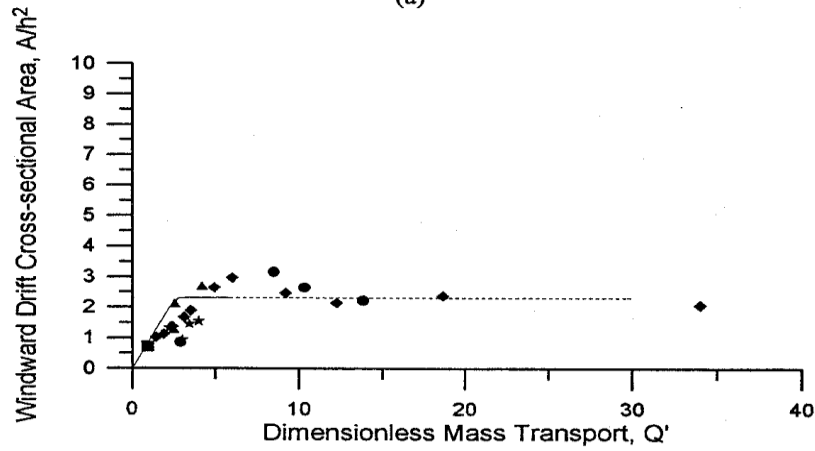
Figure 2. Profiles of the field and model drifts for a solid fence: (a) is the windward drift and (b) is the leeward drift. The wind direction is from left to right.

We can readily determine the capture efficiency of the fence at any point in time by determining the slope of the line in the plots in figure 3. We see in figure 2b that initially the capture efficiency of the windward drift in the model is greater than the field (95% versus 53%, respectively). Thus, almost no snow is available to allow development of the lee drift until the windward drift reaches saturation ( $Q' \sim 3$ ).

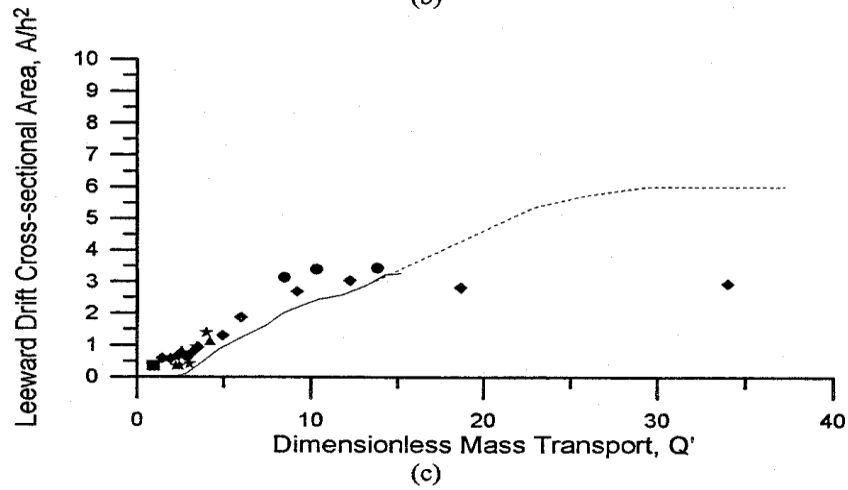
A possible reason for the distortion in capture efficiency of the windward wake in the model compared to the field could be a result of a difference in the transported snow concentration with height between model and prototype. We observed that a significant amount of snow was being transported over the 1.2 m solid fence in the field at wind speeds greater than 10m/s. However, most of the blowing snow in the wind tunnel occurred in a layer 1 - 3cm thick,



(a)



(b)



(c)

Figure 3. Plot of drift area versus snow mass transport. (a) is the total drift area, (b) windward drift area and (c) leeward drift area.

with very little transport being carried above the 10.4cm fence. This may reflect the fact that we reduced the ratio of wind speed to threshold wind ( $U/U_t$ ) speed to minimize Froude number distortion. As previously stated,  $U/U_t$  in the model was 1.25, while in the field it was about 2 - 3. It is generally recognized that this parameter and the ratio of particle fall velocity to threshold velocity need to be preserved to maintain similitude of drift concentration with height between model and prototype. Essentially all the snow transport in the model can interact with the windward separation pocket, increasing the development rate of the windward drift as compared to the field case.

Once the model leeward drift began to develop, it did so at about the same rate as the field (the capture efficiencies for the model and field were 0.25 and 0.29, respectively, see fig. 3c). However, the model drift was about twice as long as the field drift (fig. 2b). The model leeward drift length is about equal to the length of the leeward wake, 13 - 16h (Holbom 1980). We are not sure why the field drift is about half the length of the wake since it should be possible for snow to be trapped in the unfilled wake area. Note that the slope on the leeward side of the field drift is only about  $12^\circ$ , so that the model drift is not limited by the angle of repose of the glass beads.

From Owen (1964) we may estimate the trajectory height and length of a saltating particle as a function of fluid velocity and density, and particle size and density. For snow, a typical particle (density of 0.9 g/cc, 150  $\mu\text{m}$  in diameter) in a free stream wind of about 10 - 15 m/s would rise 2 - 6cm into the air and travel 20 - 60 cm down stream before landing. The height of this trajectory is about 5% of the height of the fence. Similarly the length of the trajectory is also about 4% of the length of the wake region. In contrast, the model particle (density of 2.44 g/cc, 80  $\mu\text{m}$  in diameter) driven by a free stream wind velocity of about 5 m/s has a particle trajectory that is 1 - 3cm high or about 30% of the height of the model fence. Similarly, the trajectory length is about 20% of the length of the wake region. Thus we see, the saltating model particles, in general, are carried much further down stream relative to the field. It is likely that this distortion in particle trajectory length is the cause of the longer leeward drift exhibited in the model as compared to the field. This reflects distortion in the model Froude number and possibly particle drag coefficient. However, it may be possible to reduce the effects of this distortion via changes in test conditions, and we are exploring several possible changes.

#### CONCLUSIONS

Field data of snowdrift development on a 1.22m solid fence were gathered over two winters in Wyoming. Both drift geometry, and the incident snow transport were measured during drift development. The incident flow field was also measured. Two of five drifting events were of long enough duration to achieve an equilibrium drift on the solid fence. The field drift geometry and development rate were quite repeatable, with very little scatter in the data.

A 1:12 scale model of the field solid fence was run in CRREL's Environmental Wind Tunnel. The results of this initial test showed generally good agreement between the field and model drift geometries. However, we found that windward and leeward drift development rates between model and prototype were not well preserved and that the leeward model drift tended to be long in comparison to the field. Model distortion of the blowing snow concentration with height and particle trajectory lengths probably cause these differences.

We tested the solid fence specifically to expose model distortions, and further work should yield ways to minimize their impacts. The key to optimizing the model is the availability of high quality field data. The data obtained in this current study should greatly assist development of modeling techniques for time dependent snow drift evolution.

#### ACKNOWLEDGMENTS

This work was funded by the US Army, Combat Engineering program work unit number AT42-CS-C12, "Effective Snow Management." We recognize the help of Christopher Donnelly and Jesse Stanley and in making the wind tunnel model and collecting the model data.

#### REFERENCES

- Anno, Y. (1984) "Requirements for modeling a snowdrift," *Cold regions science and technology*, **8**, 241-252.  
Haehnel, R.B. and Lever, J.H. (in press) "Field measurements of snow drifts," *Proceedings of ASCE/ISSW Workshop on the physical modelling of wind transport of snow and sand*, Snowbird, UT, November, 1994.  
Haehnel, R.B., Wilkinson, J.H., and Lever, J.H. (1993) "Snowdrift modeling in the CRREL wind tunnel," *Proceedings of the 50<sup>th</sup> Eastern Snow Conference*, Quebec City, Quebec, 139-147.

- Holmbom, A. (1980) *Boundary layer flow over different two-dimensional obstacles*, Research Report Series A, No. 59, Division of Water Resources Engineering, University of Lulea, Sweden.
- Isyumov, N. Mikitiuk, M. and Cookson, P. (1989) "Wind tunnel modeling of snow drifting: applications to snow fences," in M. Ferrick and T. Pangburn (Eds.), *Proceeding, 1<sup>st</sup> International Conference on Snow Engineering, Santa Barbara, CA, CRREL Special Report 89-6*, 210-226.
- Iversen, J.D. (1979) "Drifting snow similitude," *J. Hydr. Div. ASCE*, **105**, No. HY6, 737-753.
- Iversen, J.D. (1980) "Drifting snow similitude—transport-rate and roughness modeling," *J. Glaciol.*, **26**, 393-403.
- Kind, R.J. (1976) "A critical examination of the requirements for model simulation of wind-induced erosion/deposition phenomenon such as snow drifting," *Atmos. Environ.*, **10**, 219-227.
- Kind, R.J. (1986) "Snowdrifting: a review of modeling methods," *Cold Regions Sci. Technol.*, **12**, 217-228.
- Kwok, K.C.S., Kim, D.H., Smedley, D.H., and Rohde, H.F. (1992) "Snowdrift around buildings for Antarctic environment," *J. Wind Eng. Ind. Aerodyn.*, **41-44**, 2797-2808.
- Lever, J.H. and Haehnel, R. (1995) "Scaling snowdrift development rate," *Hydr. Proc.*, **9**, 935-946.
- Mellor, M. (1965) "Blowing snow," *Cold Regions Science and Engineering Monograph Part III, Section A3c*, US Army Cold Regions Research and Engineering Laboratory, Hanover, NH.
- Odar, F. (1965) "Simulation of drifting snow," *CRREL Res. Rep. 174*, Cold Regions Research and Engineering Laboratory, Hanover, NH.
- Owen, P.R. (1964) "Saltation of uniform grains in air," *J. Fluid Mech.*, **20**, part 2, 225-242.
- Smedley, D.H., Kwok, K.C.S., and Kim, D.H., (1993) "Snowdrifting simulation around Davis Station Workshop, Antarctica," *J. Wind Eng. Ind. Aerodyn.*, **50**, 153-162.
- Strom, G.H. Kelly, G.R., Keitz, E.L., and Weiss, R.F., (1962) "Scale model studies on snow drifting," *Res. Rep. 73*, US Army Snow, Ice and Permafrost Research Establishment (now CRREL, Hanover).
- Tabler, R.D., and Jairell, R.L. (1993) "Trapping efficiency of snow fences and implications for system design," *Transportation Res. Rep. No. 1387, Snow Removal and Ice Control Technology*, 108-114.
- Weubben, J.L. (1978) "A hydraulic model investigation of drifting snow," *CRREL Rep. 76-16*, Cold Regions Research and Engineering Laboratory, Hanover, NH.